

E- and B-modes from the magnetized filamentary structure of the interstellar medium

Planck intermediate results. XXXVIII,
A&A accepted, arXiv 1505.02779

Tuhin Ghosh
IAS, Orsay

ON BEHALF OF THE PLANCK COLLABORATION

Magnetic fields in the Universe V

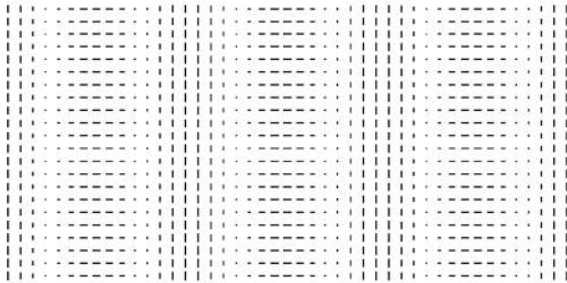
From laboratory and Stars to primordial structures

Friday 09 October 2015

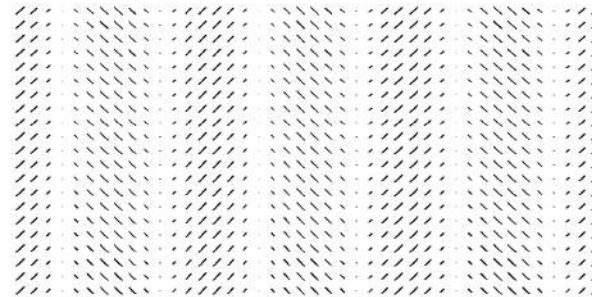


E- and B-modes in a nutshell

E-Mode Polarization Pattern



B-Mode Polarization Pattern



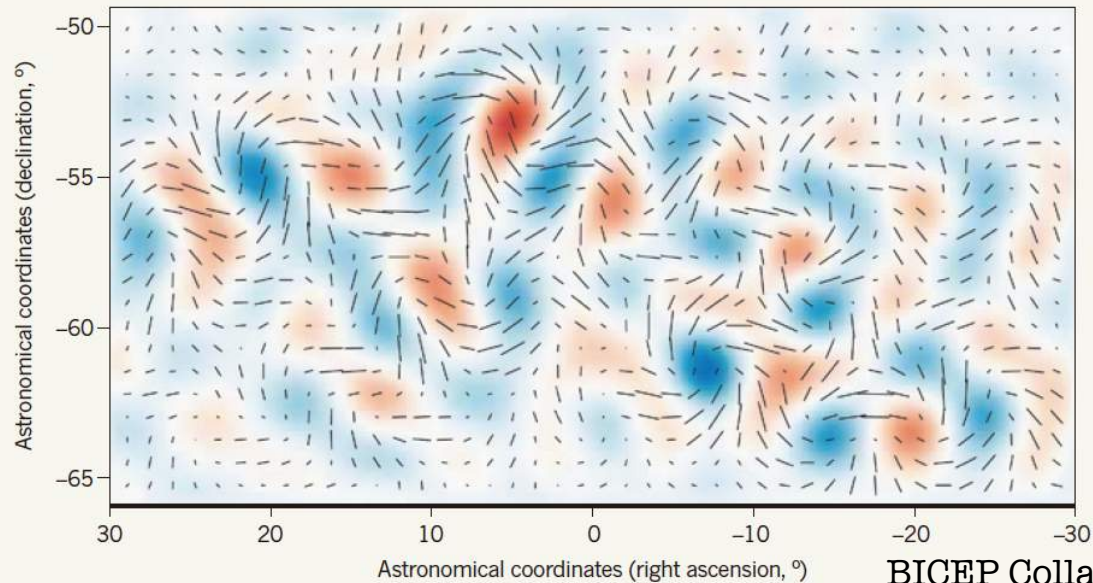
COSMIC CURL

The BICEP2 instrument observed a faint but distinctive twisting pattern, or spin, known as a curl or B-mode, in the polarization of the cosmic microwave background. This is the first evidence for gravitational waves generated by rapid inflation of the Universe some 13.8 billion years ago.

Spin intensity

■ Clockwise ■ Anti-clockwise

∖ Polarization strength and orientation at different spots on the sky.



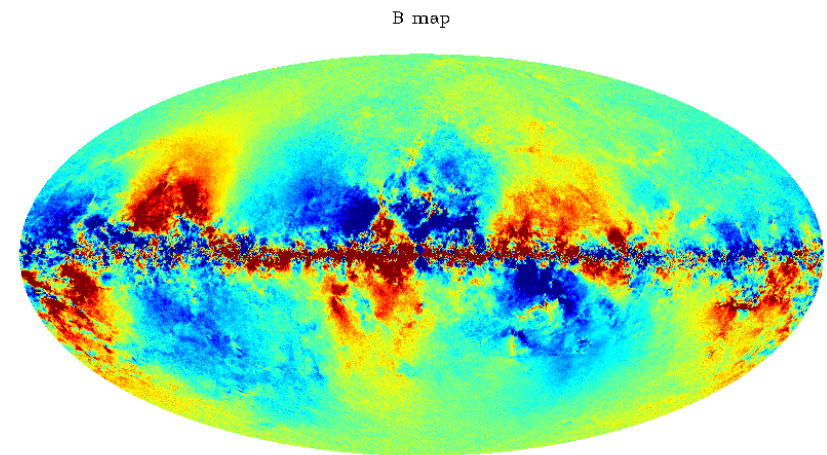
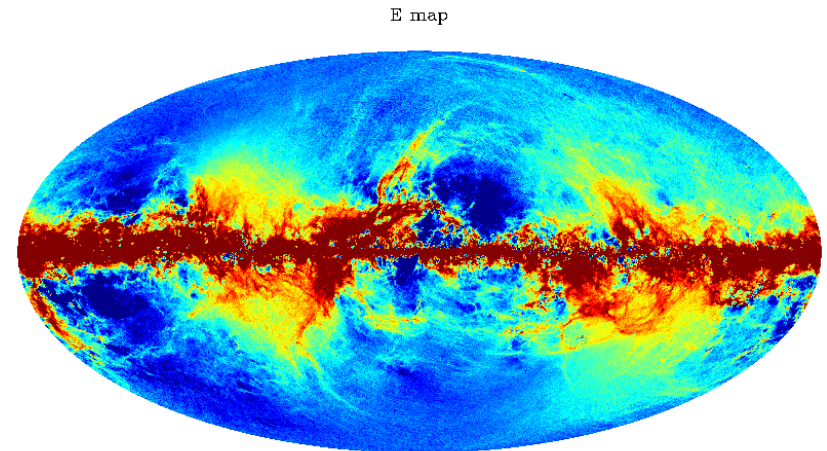
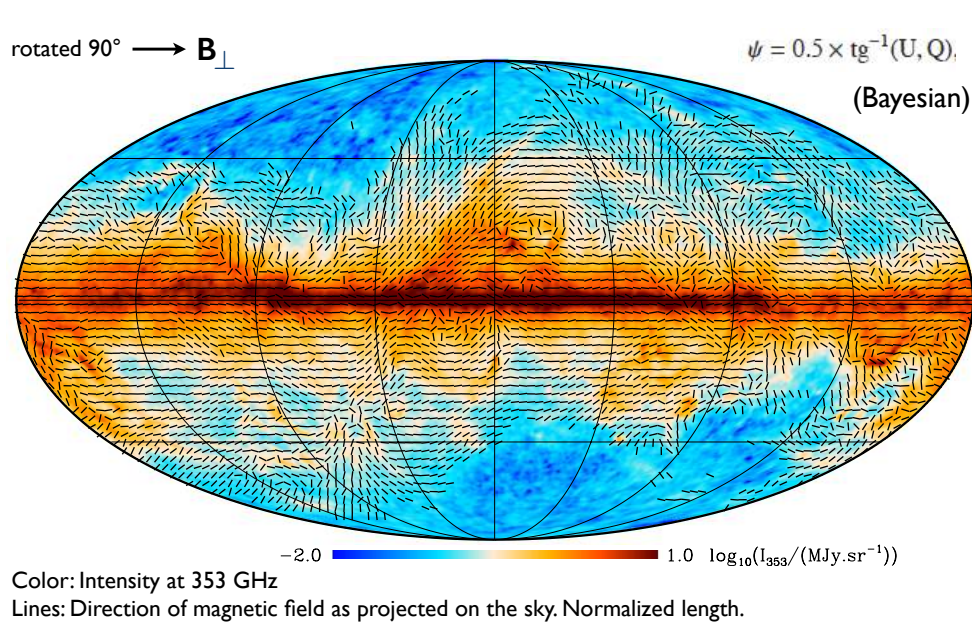
BICEP Collaboration 2014, PRL, 112



B-mode is nothing to do with the magnetic field



The Planck polarization sky

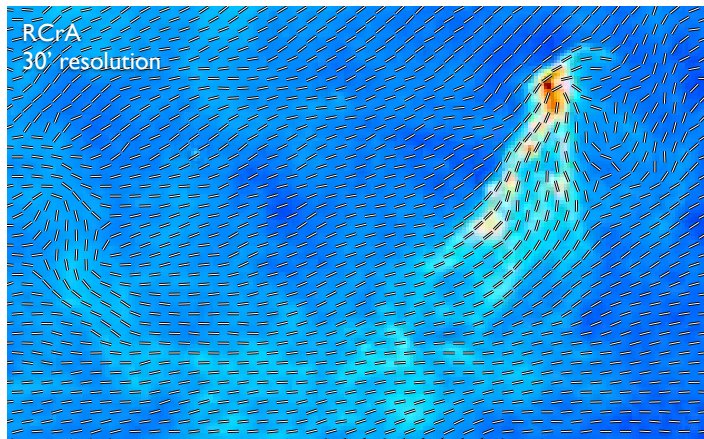
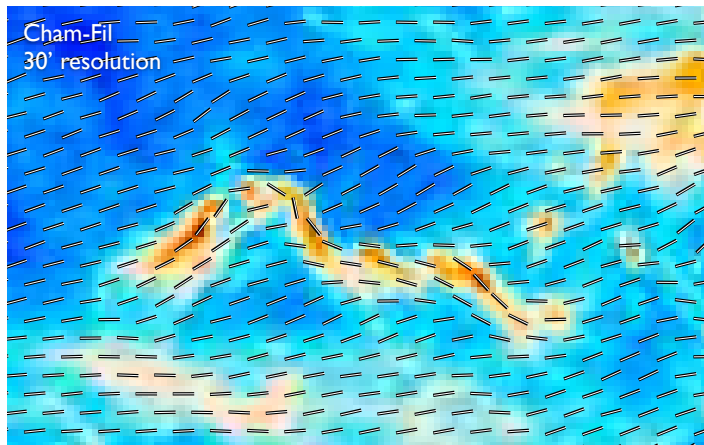


- First all-sky map of dust polarization.
- Complementary to observations of stellar polarization which provide detailed information on smaller angular scales

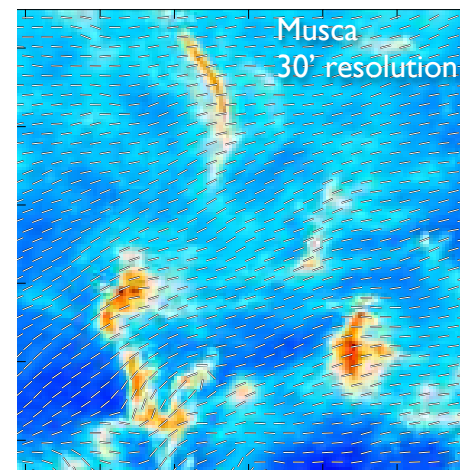
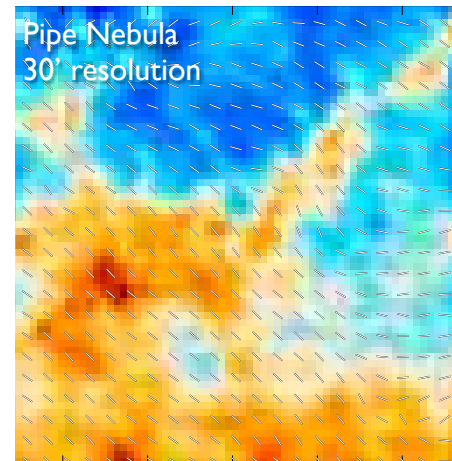


The Planck polarization sky

Magnetic field follow filaments

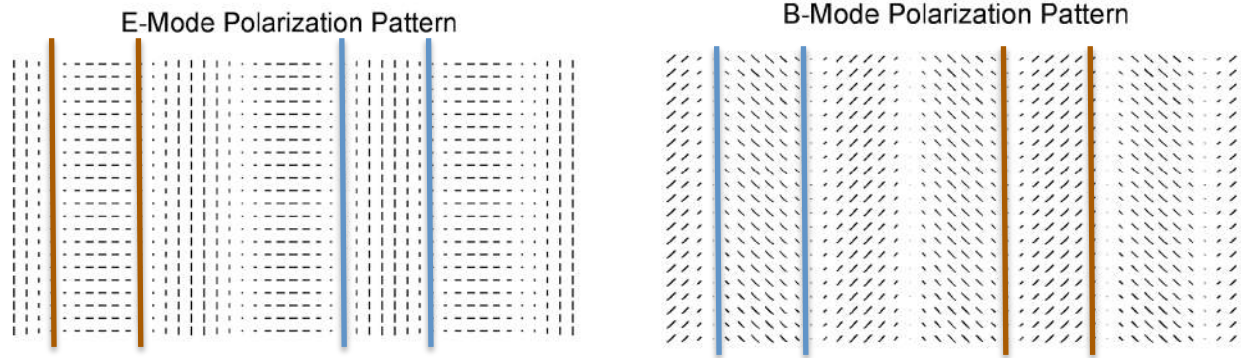


Magnetic field perpendicular to filaments



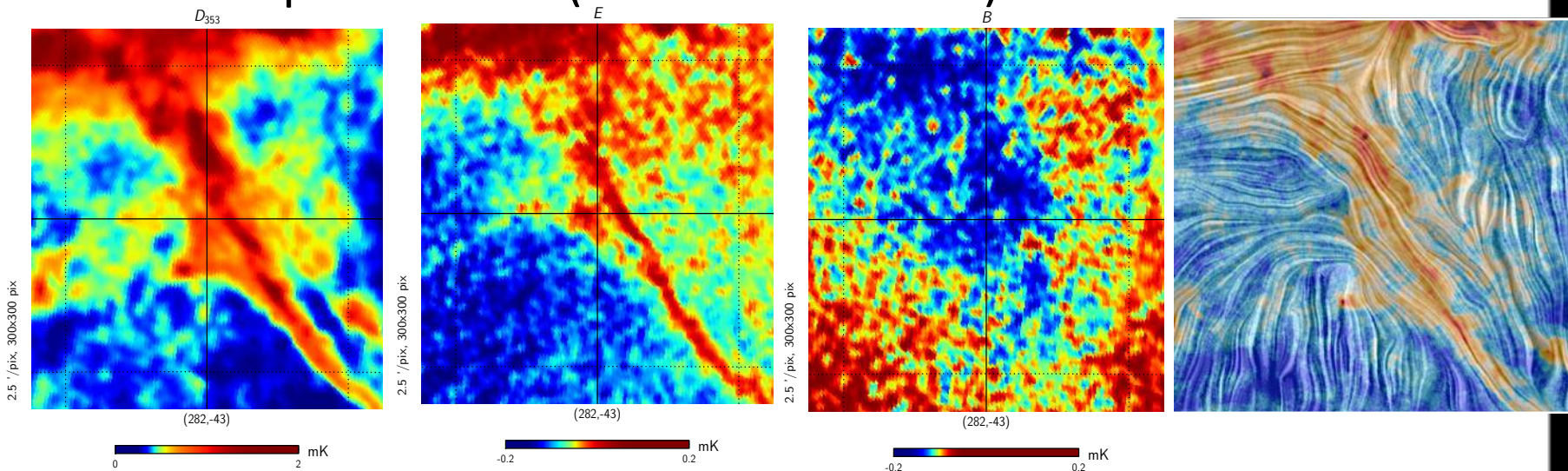


E- and B-modes in filaments



Zaldarriaga, PRD 64, 2001

Example filament (raw 353 GHz data)

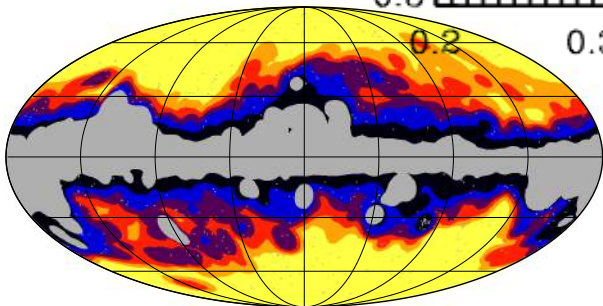
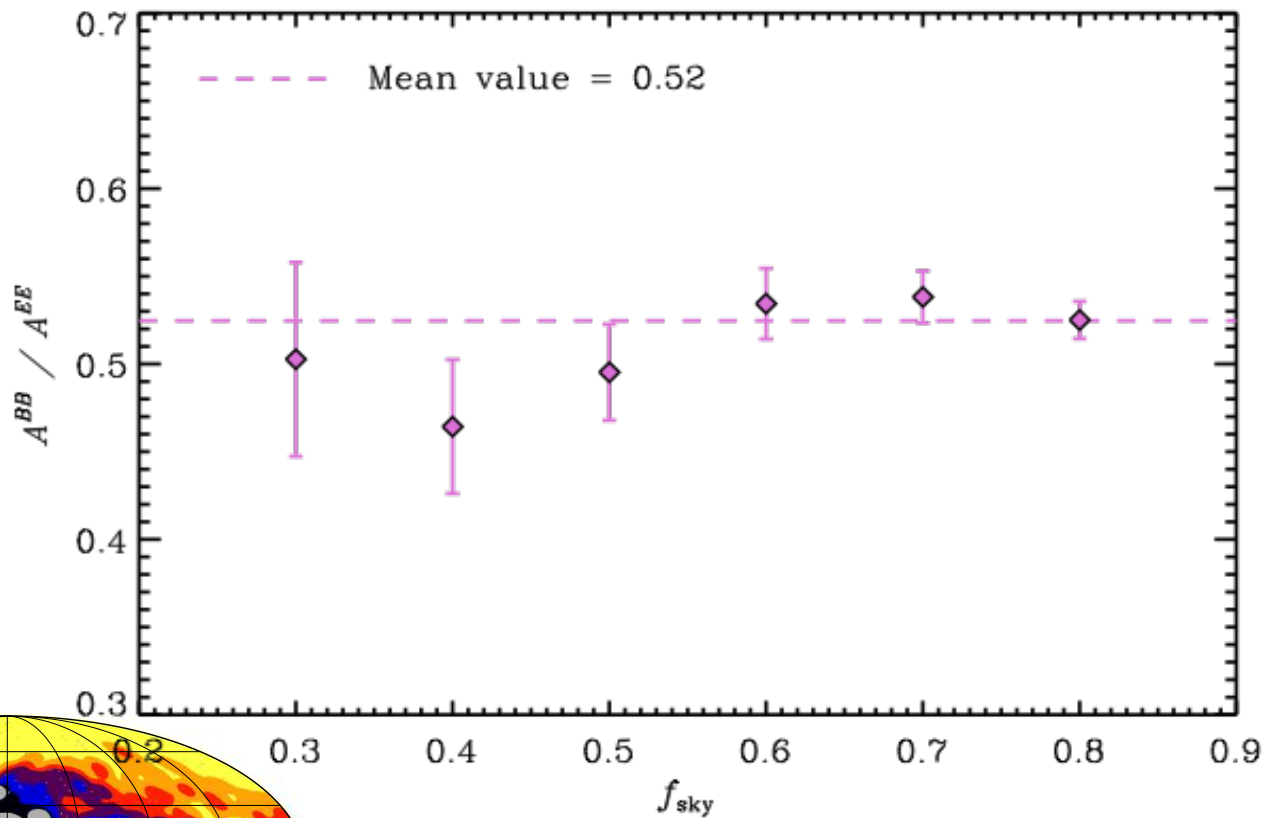


If a filament is preferentially aligned with the local direction of magnetic field, it produces more E-mode than B-mode.



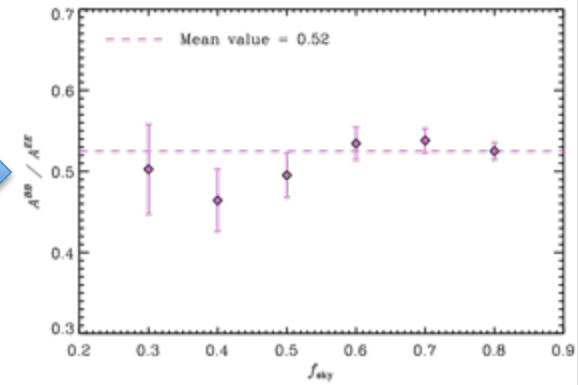
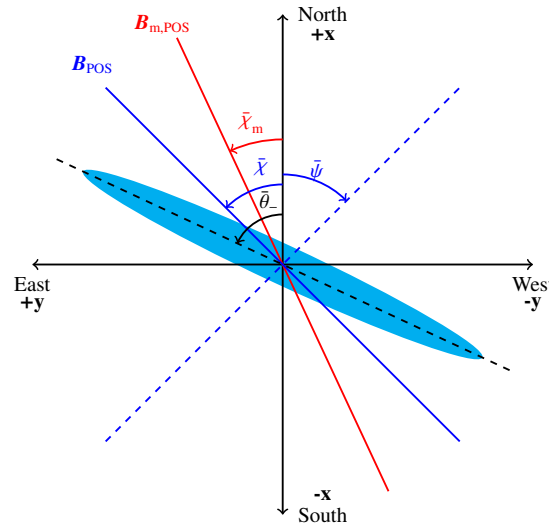
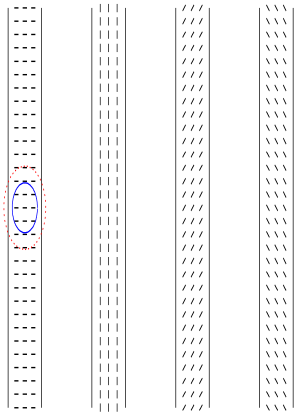
Power asymmetry in the dust E- and B-modes

Polarized dust emission produces about half as much as *B*-mode power as *E*-mode power.





Origin of dust E-B power asymmetry



Identifying elongated straight filaments

Study the relative orientation between the filaments and the magnetic field

$BB/EE \sim 1/2$



Filament-finding algorithm

Planck XXXVIII 2015, arXiv 1505.02779

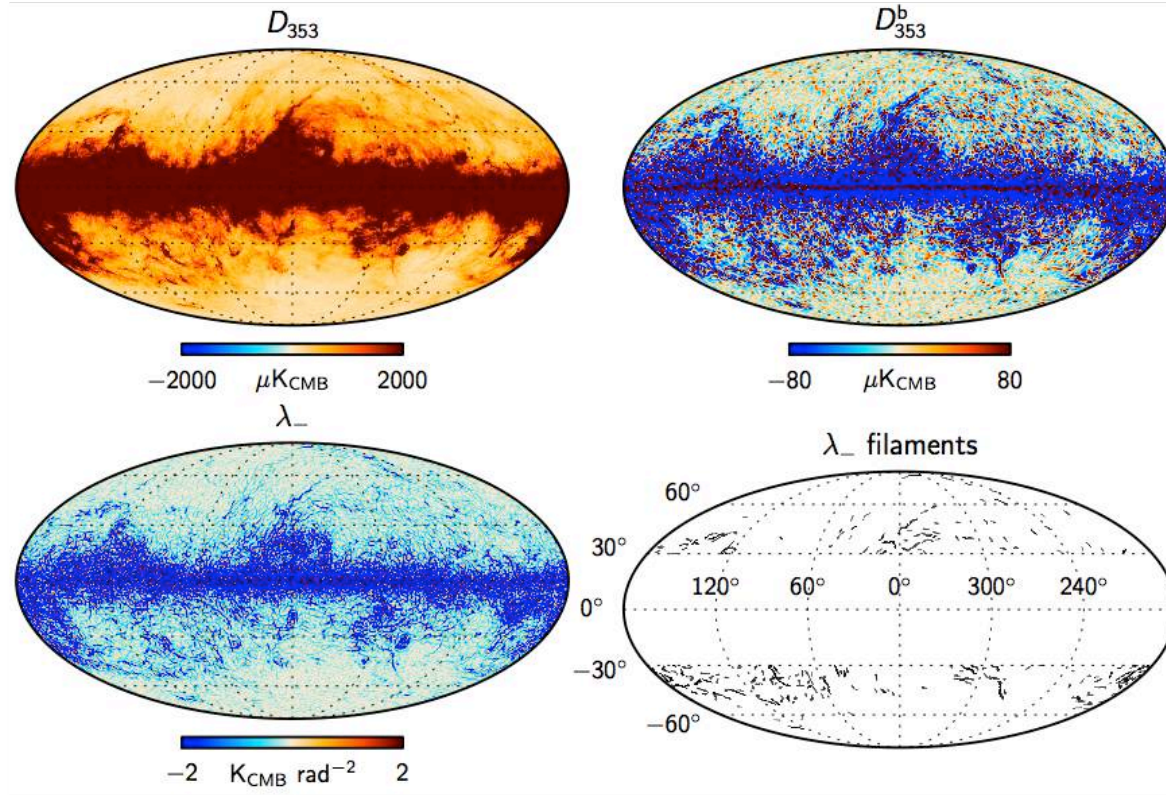


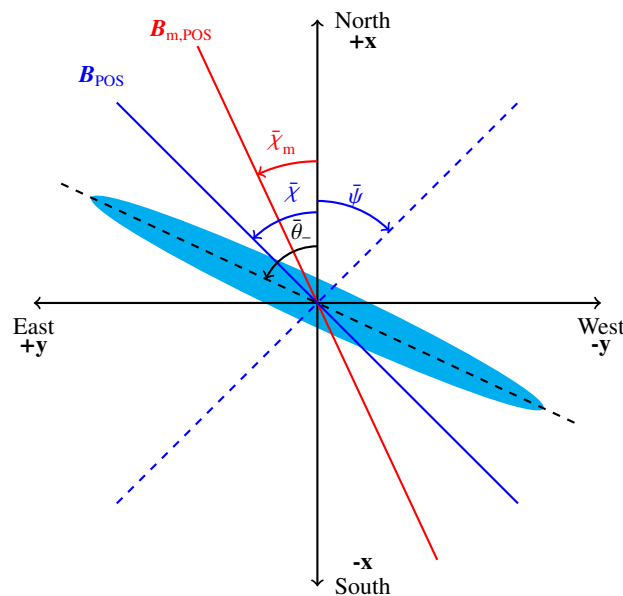
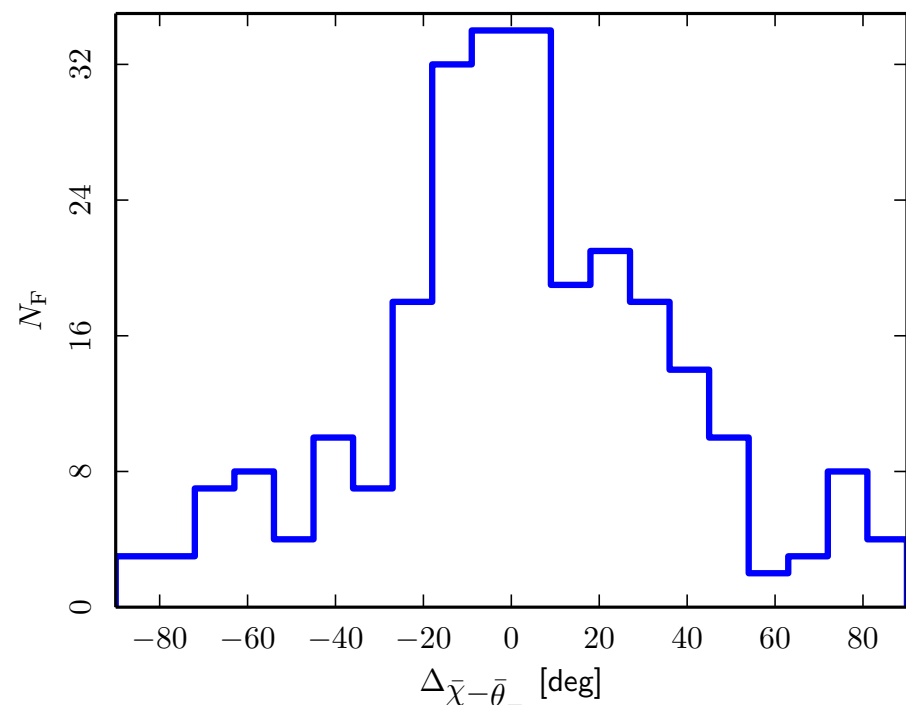
Fig. 2. Data processing steps implemented to identify filaments from the *Planck* data. We start with the *Planck* D_{353} map (upper left panel) smoothed at $15'$ resolution. The bandpass-filtered D_{353}^b map (upper right panel) is produced using the spline wavelet decomposition, retaining only the scales between $\ell = 30$ and 300 . The lower eigenvalue map of the Hessian matrix, λ_- , is shown in the lower left panel. Structures identified in the high-latitude sky λ_- map are shown in the lower right panel. The superimposed graticule is plotted in each image and labelled only on the lower right panel. It shows lines of constant longitude separated by 60° and lines of constant latitude separated by 30° . The same graticule is used in all plots of the paper.

Bond et al. 2010

- 259 filaments at high Galactic latitude ($|b| > 30^\circ$) with comparable column densities.
- Filaments have typical lengths larger or equal to 2 deg (corresponding to 3.5 pc length for a typical distance of 100 pc).



Histogram of relative orientation (HRO) between the filaments and \mathcal{B}_{POS}



- Filaments are statistically aligned with \mathcal{B}_{POS} in the high-latitude sky .
- The HRO is fitted well with a Gaussian plus a constant. The constant arises from the projection of the magnetic field and filament orientation on the plane of the sky (Planck XXXII 2014, arXiv:1409.6728).



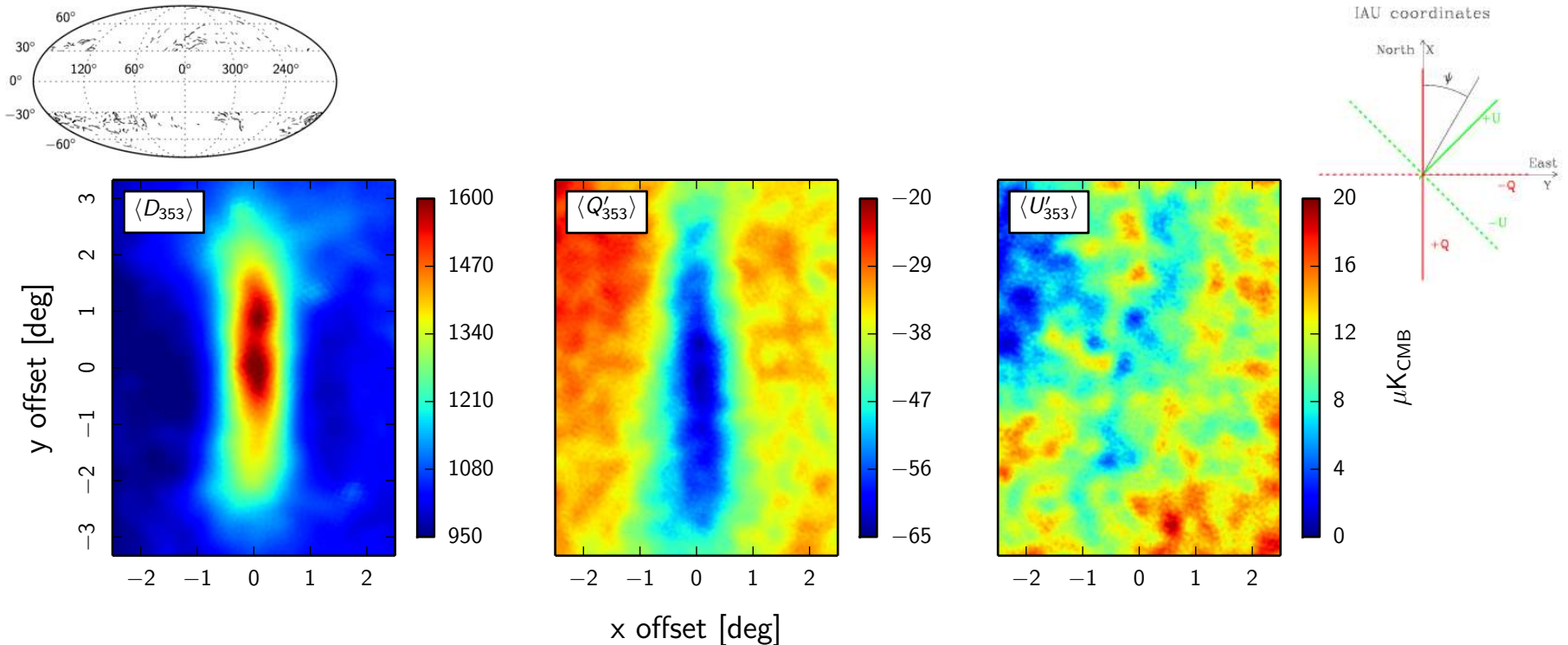
Projection effects



Projection effects (3D to 2D) are crucial for the interpretation of the shape of the distribution.



Stacking of filaments in our sample

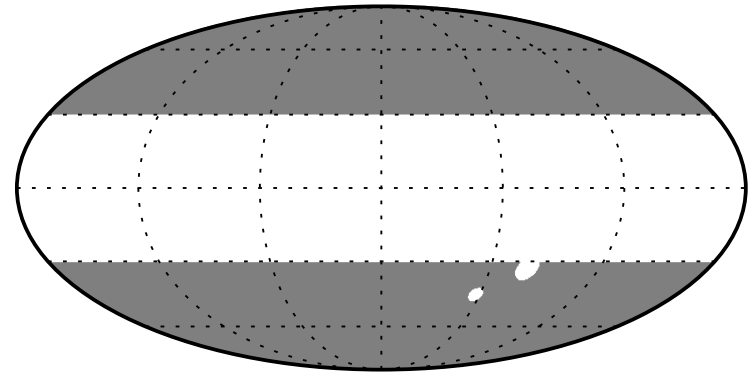


- Q' and U' are the Stokes Q and U maps computed with respect to the axis of the filament.
- The average filament appears as a negative feature with respect to the background in $\langle Q' \rangle$ image and is not seen in $\langle U' \rangle$ image.
- The 1 sigma uncertainty on the $\langle Q' \rangle$ and $\langle U' \rangle$ images is $1.3 \mu K_{\text{CMB}}$.
- The homogeneous background in the $\langle Q' \rangle$ and $\langle U' \rangle$ images reflects the smoothness of B_{POS} over the patch size of 7×5 square degrees.
- The mean polarization fraction of the dust emission in these intensity filaments is 11%.



BB/EE variance ratio using filtered data

High-latitude sky



$$V^{EE}(\text{HL}) = \frac{1}{N_{\text{HL}}} \sum_{i=1}^{N_{\text{HL}}} E_{353,\text{HM1}}^b E_{353,\text{HM2}}^b = (46.6 \pm 1.1) \mu\text{K}_{\text{CMB}}^2,$$

$$V^{BB}(\text{HL}) = \frac{1}{N_{\text{HL}}} \sum_{i=1}^{N_{\text{HL}}} B_{353,\text{HM1}}^b B_{353,\text{HM2}}^b = (29.1 \pm 1.0) \mu\text{K}_{\text{CMB}}^2,$$

$$\frac{V^{BB}(\text{HL})}{V^{EE}(\text{HL})} = 0.62 \pm 0.03$$

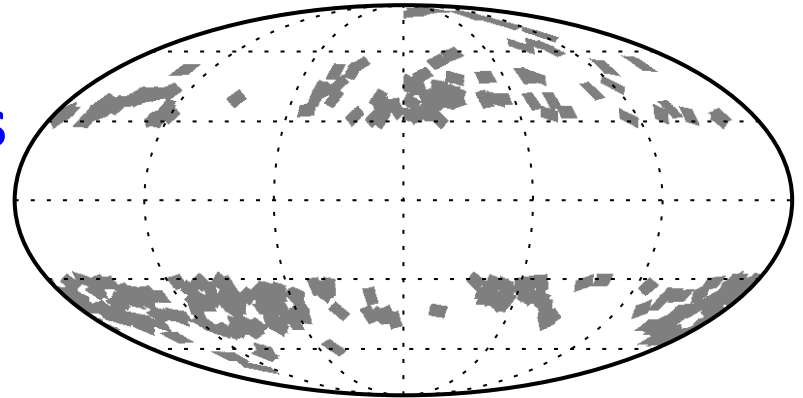
This ratio is computed over the angular scales $30 < l < 300$.

The 1 sigma errorbar on the variance estimate is computed using the cross-product of the independent subsets of the Planck data.



Filaments and their surroundings

$$(f_1 = f_{\text{sky}} = 0.28)$$



$$V^{EE}(\text{SP}) = \frac{1}{N_{\text{SP}}} \sum_{i=1}^{N_{\text{SP}}} E_{353,\text{HM1}}^b E_{353,\text{HM2}}^b = (137.5 \pm 1.4) \mu\text{K}_{\text{CMB}}^2,$$

$$V^{BB}(\text{SP}) = \frac{1}{N_{\text{SP}}} \sum_{i=1}^{N_{\text{SP}}} B_{353,\text{HM1}}^b B_{353,\text{HM2}}^b = (91.2 \pm 1.3) \mu\text{K}_{\text{CMB}}^2,$$

$$\frac{V^{BB}(\text{SP})}{V^{EE}(\text{SP})} = 0.66 \pm 0.01$$

This ratio is computed over the angular scales $30 < l < 300$.

The 1 sigma errorbar on the variance estimate is computed using the cross-product of the independent subsets of the Planck data.



Sky variance from the bright filaments

High-latitude sky:

$$V^{EE}(\text{HL}) = 46.6 \mu\text{K}_{\text{CMB}}^2$$

Filaments and their surroundings ($f_1=0.28$):

$$V^{EE}(\text{SP}) = 137.5 \mu\text{K}_{\text{CMB}}^2$$

The ratio of the sky variance is

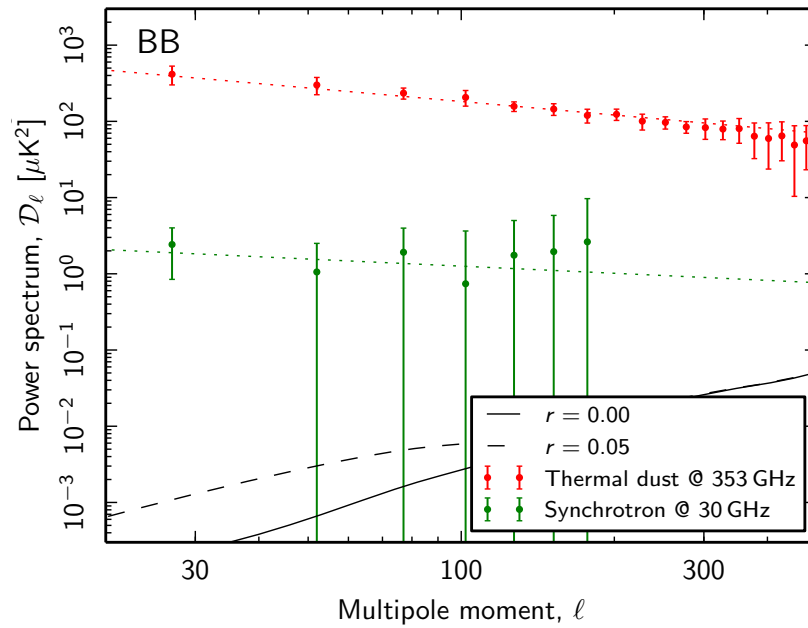
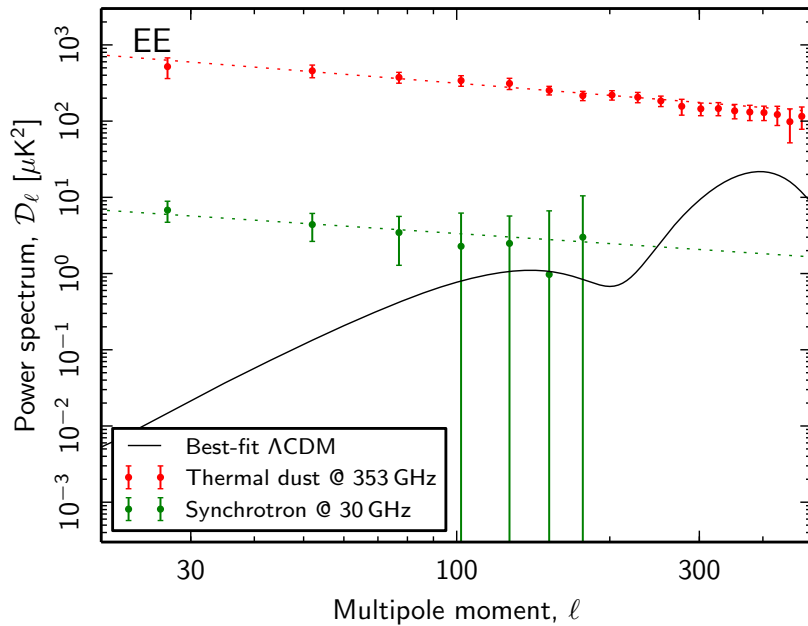
$$R_{\text{SP}} = \frac{f_1 \times V^{EE}(\text{SP})}{V^{EE}(\text{HL})} = 0.83 .$$

83 % of the total variance in EE polarization is in the bright dust intensity filaments.

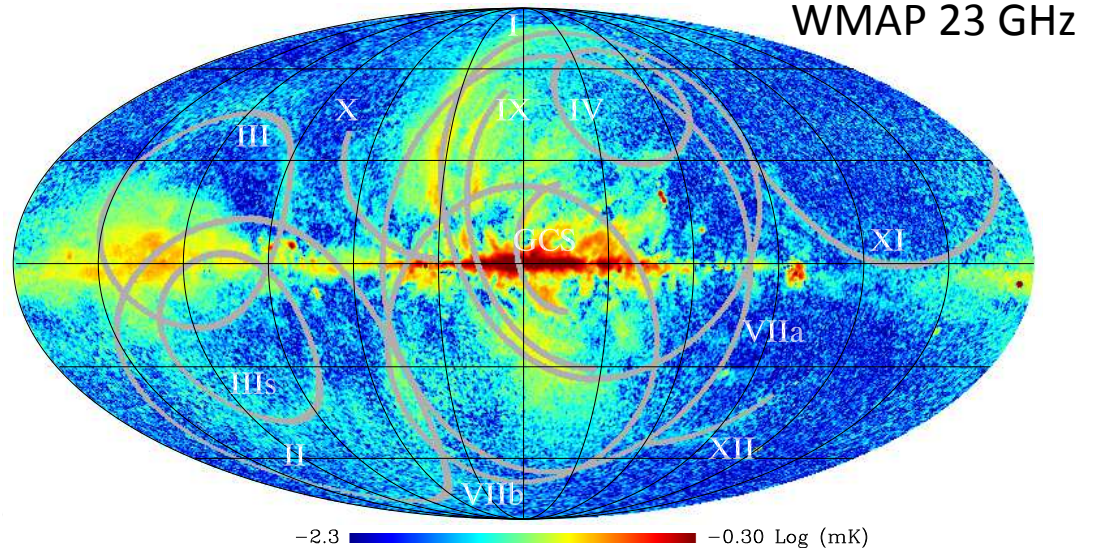
- Rest of the high-latitude latitude sky ($1-f_1=0.72$) does not contribute much to the sky variance. It includes structures like local dispersion of the polarization angle.



Synchrotron polarization



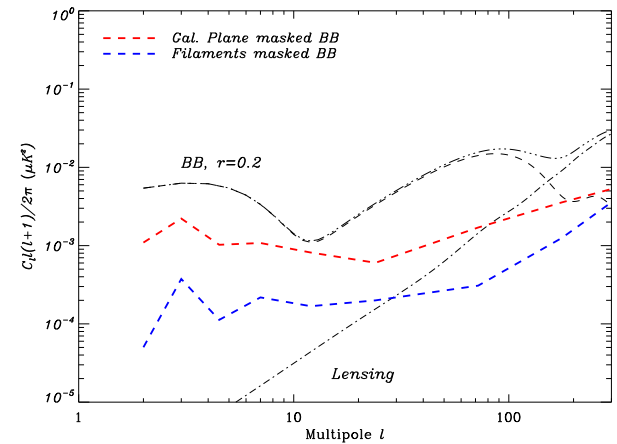
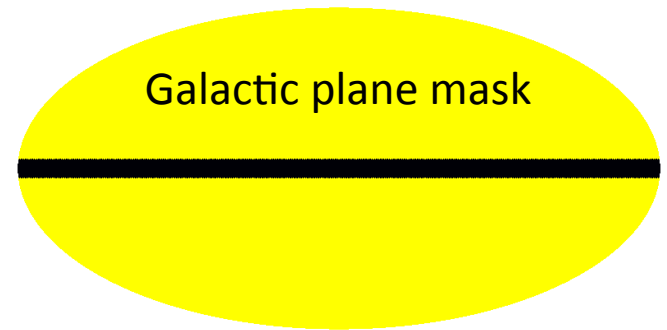
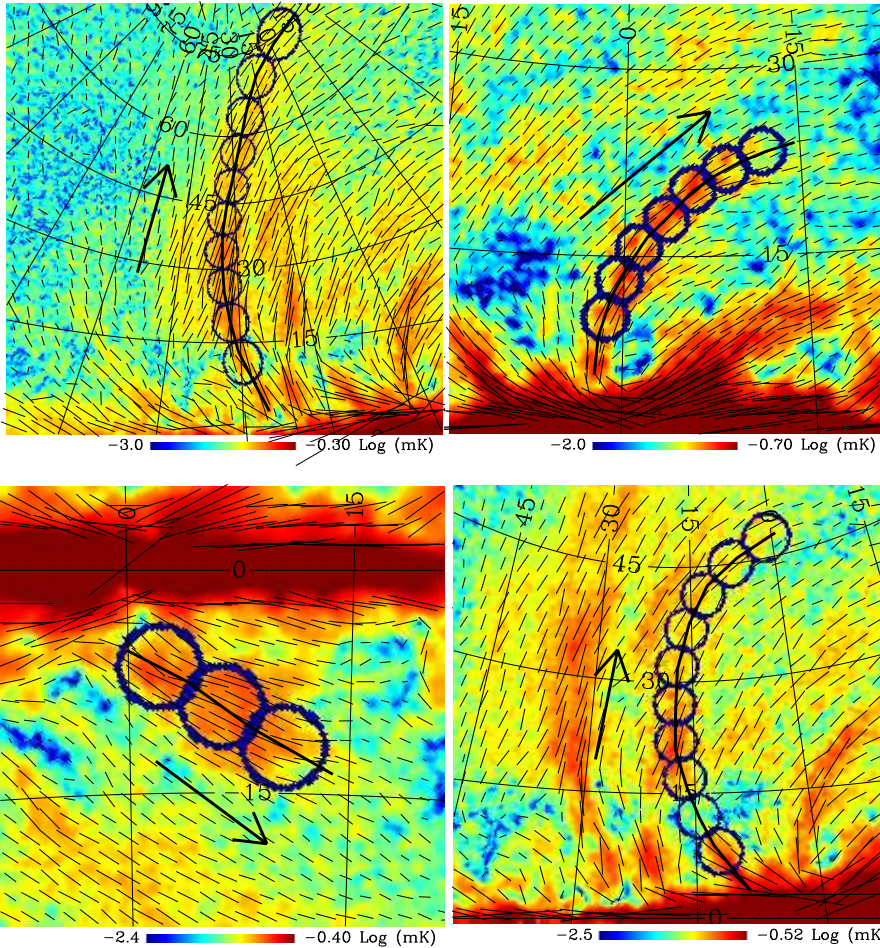
BB/EE ~ 0.36





Synchrotron polarization

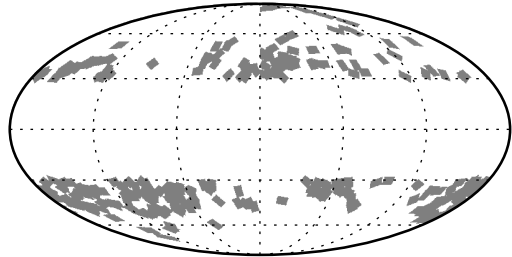
Filaments/part of loops



Strong alignment between the filaments in the synchrotron emission and the magnetic field



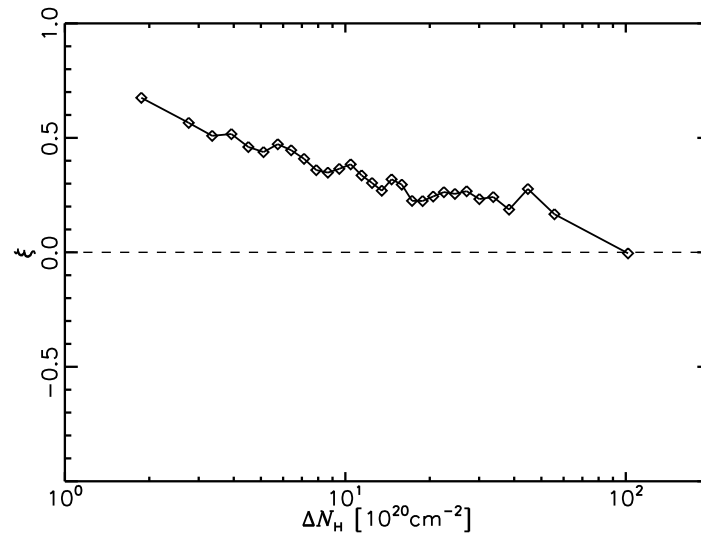
Overall picture



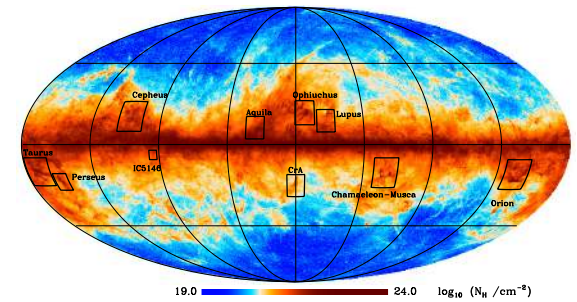
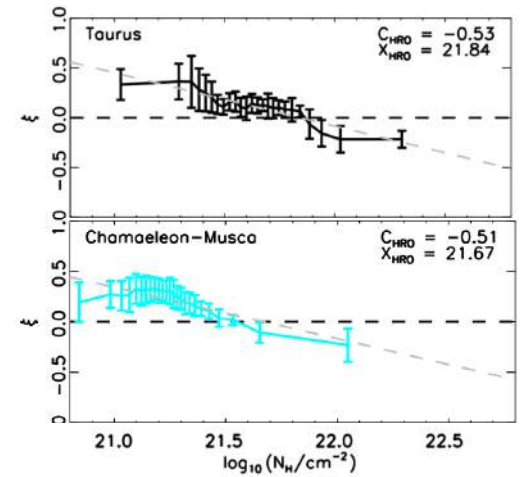
Diffuse ISM

Planck XXXVIII 2015,
arXiv 1505.02779

degree of alignment vs column density



Planck XXXII 2015,
arXiv 1409.0678



Molecular clouds

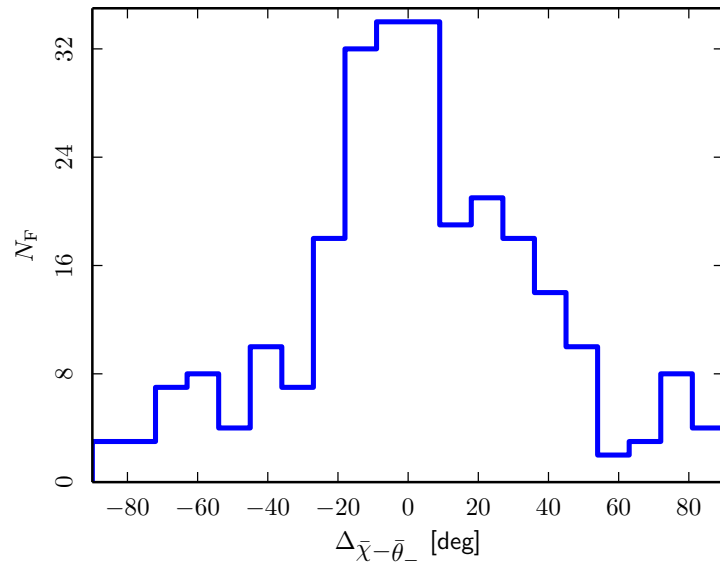
Planck XXXV 2015,
arXiv 1502.04123

Degree of alignment is:
equal to 1 in case of perfect alignment
equal to -1 in case of perfect perpendicularity



Conclusions

- Filaments in the diffuse medium are **statistically aligned** with the local magnetic field.
- The mean polarization fraction of the dust emission in the filaments of diffuse interstellar medium is **11%**.
- The histogram of relative orientation between the bright filaments and the local magnetic field can explain the **observed E-B power asymmetry**.
- Future models of dust polarization need to take into account the **alignment between the filaments and the magnetic field**.
(See poster by Flavien Vansyngel)



The scientific results that we present today are a product of the **Planck Collaboration**, including individuals from more than **100 scientific institutes in Europe, the USA and Canada**



Planck is a project of the European Space Agency, with instruments provided by two scientific Consortia funded by ESA member states (in particular the lead countries: France and Italy) with contributions from NASA (USA), and telescope reflectors provided in a collaboration between ESA and a scientific Consortium led and funded by Denmark.